Evidence of Nonaffine and Inhomogeneous Deformation of Network Chains in Strained Rubber-Elastic Networks by Deuterium Magnetic Resonance†

Wolfram Gronski,* Reimund Stadler, and Marly Maldaner Jacobi‡

Institut für Makromolekulare Chemie der Universität Freiburg, D-7800 Freiburg, Federal Republic of Germany. *Received August 15, 1983*

ABSTRACT: The segmental orientation of uniaxially strained poly(1,4-butadiene) networks was probed by deuterium magnetic resonance over a wide range of extension ratios. The experiments were performed on homogeneously deuterated networks and on partially deuterated networks with short deuterated segments at network junctions. The analysis of the strain-dependent line shapes of the deuterium resonances is interpreted in terms of a nonaffine deformation mechanism by means of which short elastically effective chains are stretched to a greater extent than long chains. Comparison of homogeneously and junction deuterated networks gives evidence of inhomogeneous deformation of individual chains with an excess orientation near network junctions.

Introduction

In recent experimental studies of rubber elasticity the mechanism of deformation and orientation of network chains has received increasing attention. This has been made possible mainly by small-angle neutron scattering (SANS), by means of which changes of global chain dimensions can be studied.[1] For the study of chain orientation on a segmental level deuterium magnetic resonance (^{2}H NMR) appears to be a most promising method. In a ^{2}H NMR study of uniaxially strained elastomers swollen in deuterated solvents, conclusions were drawn from the observed quadrupolar splitting of the solvent concerning short-range nematic-like order of chain segments.[2] Direct observation of segmental order of network chains in deuterated poly(dimethylsiloxane) networks has also been published recently.[3] The advantage of ^{2}H NMR as compared to rheooptical methods[4] rests on the possibility of introducing deuterium labels at defined sites of the network, e.g., at network junctions.[5] The study of elastomers carrying deuterated segments at cross-links is of particular interest because the nature of network junctions and of their functionality is of central importance in all molecular theories of rubber elasticity. In the "affine" theory[6] the junction points in which network chains terminate are assumed to be firmly embedded in the elastomeric matrix by virtue of constraints imposed by other spatially neighboring cross-links and entanglements and as such undergo affine displacements corresponding to the macroscopic changes of dimensions. In the "phantom" model[7,8] the junctions are assumed to fluctuate without restrictions about average positions. In this theory the mean positions are affine in the strain and the junction fluctuations are invariant. Flory[9] has proposed a modification of the "phantom network" in which the junction fluctuations are partially suppressed such that in the limits of small and large deformations affine and phantom behavior is approached, respectively. The effect of reducing junction fluctuations is to predict that chain deformation is smaller than predicted by the affine model and greater than for the phantom model, which represents the lower deformation limit.[10] Contrary to theoretical predictions, recent SANS experiments on model networks prepared by end-linked poly(dimethylsiloxane) have shown that changes of network chain dimensions are smaller than given by the affine model and, for the highest molecular weights studied, less than for the phantom limit, even at moderate extensions of the networks.[1] To explain this behavior it has been suggested that large macroscopic deformations may be possible through topological rearrangements on a scale larger than the mesh size involving only small molecular deformations.[11] This idea has been rationalized in terms of a model of network unfolding in which the nonaffine chain deformation is described by an effective microscopic extension ratio of network chains that is smaller than the macroscopic extension ratio.[10] In this model, as in the modification of the phantom model, the constratins of network junctions are considered as not perturbing the Gaussian chain statistics. This implies that the deformation of network chains between topologically neighboring junctions is homogeneous along their contour length. In the case of an inhomogeneous deformation mechanism it would be difficult to distinguish this mechanism from a network unfolding mechanism by observation of the changes of overall chain dimensions by SANS. It is the purpose of the present paper to show not only that ^{2}H NMR studies on deuterated networks provide information about the nonaffine character of network deformation but that a comparison of homogeneously deuterated networks with networks carrying deuterated segments at cross-links also gives information concerning the question as to what extent the deformation of single chains can be considered to be homogeneous along their contour length.

Background

The anisotropic interaction of the deuteron quadrupole moment with the electric field gradient tensor (EFG) of its electronic surroundings removes the degeneracy of the Zeeman energy levels, giving rise to a quadrupolar splitting of the ^{2}H NMR signal. In the case of a rigid system with specific orientation of the principal axes, in which the magnetic field B_0 is specified by the polar angles ϑ and φ, the magnitude of this splitting is given by[12]

$$\Delta\nu = \tfrac{3}{2}\delta(P_2(\cos\vartheta) + \tfrac{1}{2}\eta \sin^2\vartheta \cos 2\varphi) \qquad (1)$$

where $\delta = e^2qQ/h$ is the static quadrupolar coupling constant, η is the asymmetry parameter, and $P_2(\cos\vartheta) = {}^1/_2(3\cos^2\vartheta - 1)$ is the second Legendre polynomial. For deuterons in rigid C–D bonds the asymmetry parameter $\eta \approx 0$ and ϑ then is the angle between the C–D bond direction and B_0. The magnitude of δ is 164 kHz for polyethylene.[13] This value will also be assumed for the CD_2 groups of deuterated poly(1.4-butadiene).

In rigid systems with an orientational distribution of C–D bonds, symmetrically shaped powder spectra are obtained, the specific line shape of which contains infor-

† Dedicated to Professor W. H. Stockmayer on the occasion of his 70th birthday.

‡ On leave from the Department of Chemistry, Universidade Federal do Rio Grande do Sul, 90 000 Porto Alegre, RS, Brazil.

0024-9297/84/2217-0741$01.50/0

Table I
Characterization of the Polybutadiene Networks Studied

sample	primary mol wt/type	cross-link agent,[a] mol %	M_c swelling[b]	M_c elastic[c]
PB_d-5-4	75 000/linear	2	17 000	19 500
PB_d-3-5	115 700/linear	0.8	31 300	15 900
PB_d-3-6	115 700/linear	1.2	27 400	11 600
PB_d-Si-1	116 800/star[d]	0.6	49 400	27 000
PB_d-Si-3	116 800/star[d]	1.0	29 000	15 900

[a] 4,4'-Methylenebis(1,4-phenylene)bis-1,2,4-triazoline-3,5-dione. [b] Average molecular weight between cross-links calculated by the Flory-Rehner equation, using the finite molecular weight correction and the interaction parameter $\chi = 0.29$. [c] Average molecular weight between cross-links determined from stress-strain measurements ($2C_1$ from the Mooney-Rivlin equation). [d] 6% of each branch contains partially deuterated segments.

mation concerning the orientational distribution function. In the presence of molecular motion the NMR line shapes will change.[14] In rubbers motions are rapid with respect to the inverse width of the spectrum δ^{-1} in the absence of motion. In this rapid-exchange limit the fast local conformational modes with correlation times $\tau_c < 10^{-7}$ s lead to partially averaged quadrupolar coupling. Because of slower modes of motions, due to restrictions imposed by network junctions and entanglements, the averaging is incomplete and the residual quadrupolar coupling of the averaged EFG tensor of less than 1% of the static coupling determines the line width.[15] In an isotropic rubber all directions are sampled rapidly on the NMR scale, and a single narrow line of a few hundred hertz width with zero quadrupolar splitting is observed. In a uniaxially strained rubber the motions become anisotropic with respect to the stretching direction, with the result that the end-to-end distance of chain segments will have an orientational memory time $\tau_c > 10^{-7}$ s with respect to the preferential direction. Assuming that a certain statistical segment is of sufficient length such that the reorientation of C–D bonds and the end-to-end vector of this segment are uncorrelated, averaging over the fast modes of anisotropic motions in eq 1 yields for the quadrupolar splitting of an oriented sample by means of the addition theorem of sperical harmonics

$$\Delta\nu = {}^3/_2\delta\langle P_2(\cos\Phi)\rangle\langle P_2(\cos\vartheta)\rangle \qquad (2)$$

where ϑ is now the angle between the end-to-end vector of the statistical segment and the field direction $\vec{B}_0$ and Φ is the angle between a C–D bond and the end-to-end vector. Comparing eq 2 with eq 1, one sees that eq 2 is of the same form as for an axially symmetric averaged tensor $\overline{EFG}$ with an average coupling constant $\bar{\delta} = \delta\langle P_2(\cos\Phi)\rangle$. In order to relate the segmental orientation with respect to $\vec{B}_0$ to the orientation with respect to the stretching direction $\vec{d}$, the relation $\langle P_2(\cos\vartheta)\rangle = \langle P_2(\cos\Psi)\rangle\langle P_2(\cos\Theta)\rangle$ is inserted in eq 2, where Θ is the angle between the end-to-end vector of the statistical segment with respect to $\vec{d}$ and Ψ is the angle of $\vec{d}$ with respect to $\vec{B}_0$. For the perpendicular orientation $\vec{d} \perp \vec{B}_0$, as realized in the following experiments, the quadrupolar splitting is expressed by the segmental orientation function $\langle P_2(\cos\Theta)\rangle$ through the equation

$$\Delta\nu = {}^3/_4\delta\langle P_2(\cos\Phi)\rangle\langle P_2(\cos\Theta)\rangle \qquad (3)$$

The validity of eq 3 relies primarily on the assumption that the statistical segment is of sufficient length that the internal reorientation of C–D bonds within the statistical segment is uncorrelated with the motion of the end-to-end vector. On the other hand, the segment has to be small enough to ensure that the modes of anisotropic reorientation about the stretching direction over which the average has been taken are fast with respect to the NMR time scale both for internal motions within the segment and for the segment as a whole. This shows that the length of the statistical segment, yet to be defined, depends on the dynamical properties of the system. An essential additional requirement for the following analysis concerns the slow restricted anisotropic motions due to topological constraints of the network which are not averaged and determine the width and shape of the observed doublet of resonances. It will be assumed that the rates and nature of these slow rearrangements of the chains are independent of strain. The shape of the lines corresponding to a given segmental orientation, i.e., the quadrupolar splitting, is then simply given by the Lorentzian line of the isotropic sample.

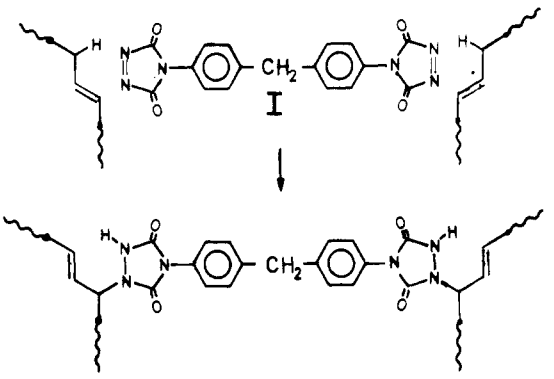

Figure 1. Cross-linking of polybutadiene with 4,4'-methylenebis(1,4-phenylene)bis-1,2,4-triazoline-3,5-dione (I) via the "double ene reaction".

Experimental Section

A. Synthesis and Characterization. Homogeneously deuterated networks were prepared by cross-linking linear poly(1,4-butadiene), partially deuterated in 1,4 positions, synthesized by anionic polymerization in cyclohexane with *n*-butyllithium as initiator. Networks with deuterated segments at network junctions were obtained from cross-linking of 4-branch star polybutadiene containing short deuterated blocks at the star center. Star polybutadiene was synthesized by sequential anionic polymerization of undeuterated and 1,4-deuterated butadiene and subsequent coupling with $SiCl_4$; ca. 6% of each branch contained butadiene units. 1,4-Deuterated butadiene was obtained by H–D exchange of butadienyl sulfone.[16] The degree of deuteration after one exchange cycle was between 40% and 60%.

As cross-linking reagent the enophilic reagent 4,4'-methylenebis(1,4-phenylene)bis-1,2,4-triazoline-3,5-dione (I) was used. It was synthesized according to literature prescriptions.[17] The structure of I and the cross-linking reaction are shown in Figure 1. Cross-linking was carried out by dissolving 1 g of polymer in 20 mL of dried benzene, adding the calculated amount of I with stirring and pouring the solution into a flat Petri dish. The solvent was evaporated over a period of 5 days until films of ca. 0.5 mm were obtained. The films showed excellent elastic properties, with reversible elongations up to 800%. Table I shows the characterization of the primary molecular weight, the concentration of the cross-linking reagent I, M_c values determined from equilibrium swelling in benzene, and the constant $2C_1$ of

the Mooney–Rivlin stress–strain relation.[18] Additional details are given elsewhere.[5]

B. Experimental Methods. Rectangular strips of 3–4-cm length and ca. 0.5-cm width were cut from the films and strained to a predefined extension ratio λ in a hand-driven extensiometer, where λ was defined by the ratio of the distance between marks on the sample after and before stretching. On the flat sides of the strained sample, two half-cylinders of 2- or 3-cm length machined from Delrin were fixed by cyanoacrylate instant adhesive. After firm contact had been ensured, the strained film was cut at the ends of the cylinder. No slippage of the sample was observed after cutting. The cylinder containing the strained sample was closely fitted into the 10-mm-diameter sample tube and put into the insert of a CXP 300 Bruker NMR spectrometer operating at a ^2H frequency of 46 MHz with a $\pi/2$ pulse of 6 μs and its 3-cm solenoid coil at right angles to the magnetic field. Measurements were made with the film surface parallel to the magnetic field. In most cases the absence of biaxial strain was tested by the invariance of the quadrupolar splitting on turning the sample tube axis coinciding with the stress direction by 90°. The applied procedure ensured a homogeneous strain in the sample. Therefore no contribution from isotropic parts of the sample to the spectra are observed. The number of accumulations varied from ca. 10^3 at $\lambda = 1$ for a homogeneously deuterated sample to 10^5 at $\lambda = 8$ in an overnight run for a sample partially deuterated at network junctions.

Analysis of Spectra

A. Statistical Segment. In order to determine the size of the statistical segment appropriate for the analysis of the ^2H NMR spectra, the average orientation $\langle P_2(\cos\Phi)\rangle_0$ of methylene C–H bonds with respect to the end-to-end vector of a chain segment of n' bonds was calculated as a function of n' for an unperturbed poly(1,4-butadiene) chain containing 50% cis- and trans-1,4 units, respectively. The calculation was performed by means of a Monte Carlo procedure. For this purpose a chain segment of n' bonds was chosen with the first bond being a bond between two methylene carbon atoms. In a first step the cis/trans configuration of the double bonds within the segment and the configuration of double bonds immediately preceding the first bond and succeeding the last bond was selected by random choice. In a second step the sequence of conformations of the bond triplets between the double bonds was statistically selected by taking into account the interdependence of bond rotations in poly(1,4-butadiene) and the appropriate statistical weights at $T = 298$ K.[19] For each sequence of configurations and conformations the end-to-end distance of the segment and the projections of all methylene C–H bonds onto the end-to-end vector were determined. This was done for a representative ensemble of segments, from which the root-mean-square distance $\langle r^2\rangle_0^{1/2}$ and the differential orientation distribution $H(\Phi)$ of C–H bond orientations were obtained. The mean value of the orientation function of methylene C–H bonds was then evaluated according to

$$\langle P_2(\cos\Phi)\rangle_0 = \frac{\int_0^\pi P_2(\cos\Phi)H(\Phi)\sin\Phi\,d\Phi}{\int_0^\pi H(\Phi)\sin\Phi\,d\Phi} \quad (4)$$

Figure 2 shows the result of the calculations. The orientation function increases from −0.5 for perpendicular orientation at $n' = 2$ toward an asymptotic value of ~−0.14. Approximately the same value was obtained by matrix methods for the preferential orientation of the axis perpendicular to the double bonds in long poly(1,4-butadiene) chains of equimolar cis/trans composition.[19]

To relate the orientation of the statistical segment $\langle P_2(\cos\Theta)\rangle$ to the macroscopic extension ratio λ, we make use of the orientation function $\langle P_2(\cos\Theta)\rangle_{KG}$ of the "affine"

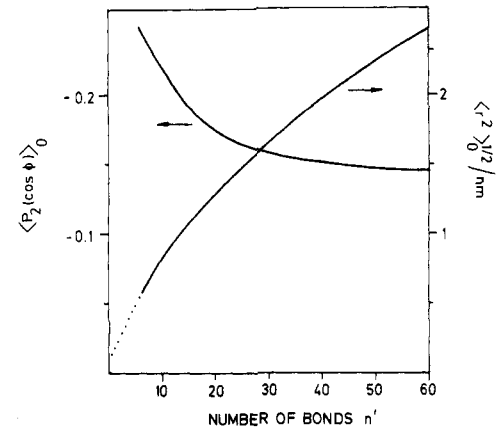

Figure 2. Root-mean-square end-to-end distance $\langle r^2\rangle_0^{1/2}$ of a chain segment of n' bonds in poly(1,4-butadiene) and orientation function $\langle P_2(\cos\Phi)\rangle_0$ of the C–H bonds of methylene groups with respect to the end-to-end vector of the segment. The curves were obtained from Monte Carlo simulations with 100 segments, with statistical weights according to ref 19. Cis content is 50%; T = 298 K.

theory of Kuhn and Grün,[20] taking into consideration the first two terms of the expansion of the inverse Langevin function to account for non-Gaussian chain statistics at high deformations[18]

$$\langle P_2(\cos\Theta)\rangle_{KG} = \frac{1}{5n}\left(\lambda^2 - \frac{1}{\lambda}\right) + \frac{2}{175n^2}\left(6\lambda^4 + 2\lambda - \frac{8}{\lambda^2}\right) + \frac{6}{875n^3}\left(10\lambda^6 + 6\lambda^3 - \frac{16}{\lambda^3}\right) + \ldots \quad (5)$$

where n is the number of statistical segments per chain. At small derformations, where Gaussian chain statistics are valid, only the first term of eq 5 makes a significant contribution, the actual deviation from Gaussian behavior depending on n. If the theoretical expression of eq 5 is inserted into eq 3, expressing the relation between segmental orientation and quadrupolar splitting, it cannot be expected that $\langle P_2(\cos\Phi)\rangle$ in eq 3 will be the true orientation factor of the methylene C–D bonds with respect to the statistical segment vector. Therefore in the following analysis, this factor will be considered as an apparent orientation parameter $\langle P_2(\cos\Phi)\rangle_{app}$ which may depend on n and λ. However, in the limit of small strain, for $\lambda \to 1$, it can be expected that $\langle P_2(\cos\Phi)\rangle_{app}$, as determined from the experimental quadrupolar splitting and the theoretical expression of eq 5, converges to the orientation factor of the unperturbed chain; i.e.

$$\langle P_2(\cos\Phi)\rangle_0 = \frac{\lim_{\lambda\to 1}\Delta\nu}{^3/_4\delta(\lim_{\lambda\to 1}\langle P_2(\cos\Theta)\rangle_{KG})} \quad (6)$$

As illustrated in Figure 2, $\langle P_2(\cos\Phi)\rangle_0$ depends on the number of bonds n' per statistical segment. The same holds for $\langle P_2(\cos\Theta)\rangle_{KG}$ since

$$n = 4M/n'M_0 \quad (7)$$

where M is the molecular weight of an elastically effective network chain and M_0 is the molecular weight of the butadiene unit. Therefore eq 6 can be used to determine the number of bonds per statistical segment from quadrupolar splittings obtained from the analysis of the NMR line shape and extrapolation to the unstrained state.

B. Distribution of Network Chain Lengths. The increasing line width and asymmetry of the two resonances of the spectral pattern with increasing extension ratio as

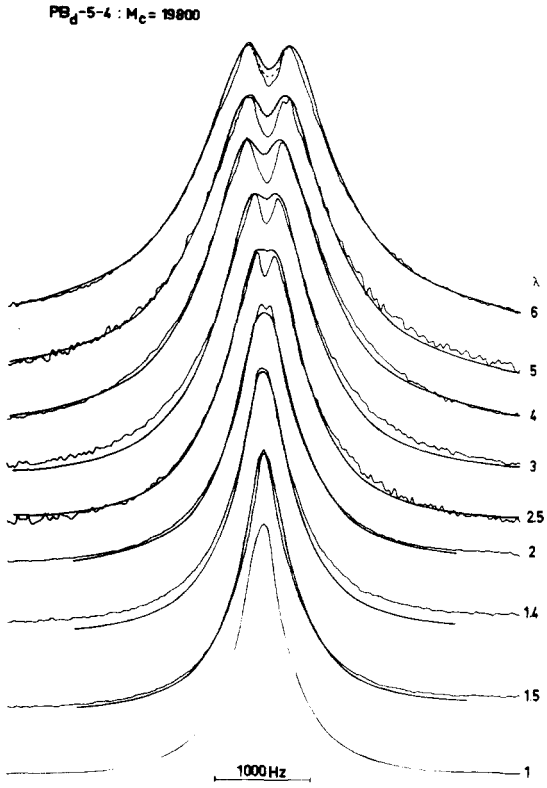

Figure 3. ^{2}H NMR spectra of sample PB_d-5-4 as a function of extension ratio λ. The smooth full curves were calculated with a most probable distribution of chain lengths with number-average molecular weight M_c and with non-Gaussian chain statistics. The dashed curve was calculated with a Gaussian distribution of chain lengths with $M_w/M_c = 1.9$.

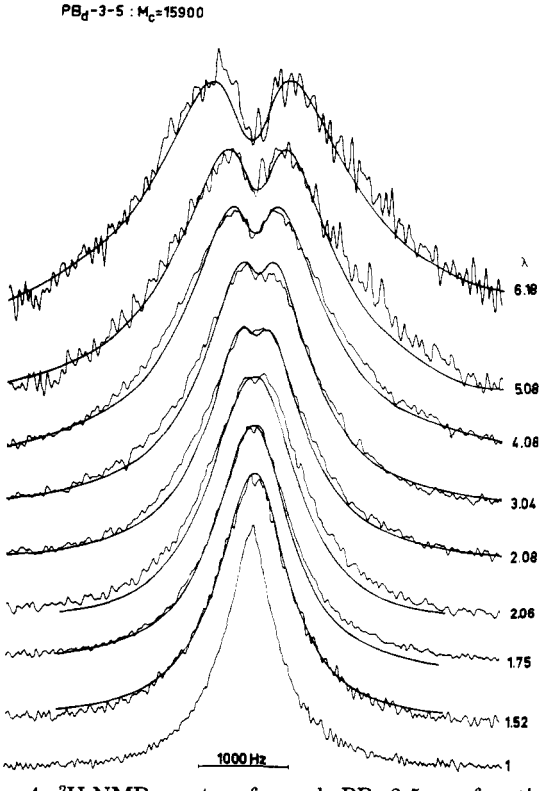

Figure 4. ^{2}H NMR spectra of sample PB_d-3-5 as a function of extension ratio λ and calculated spectra (see caption of Figure 3).

exhibited by the spectra of Figures 3–7 in the following section demonstrate that an interpretation based solely on the splitting at maximum peak height is not feasible. It is assumed that the changes of line shape have to be at-

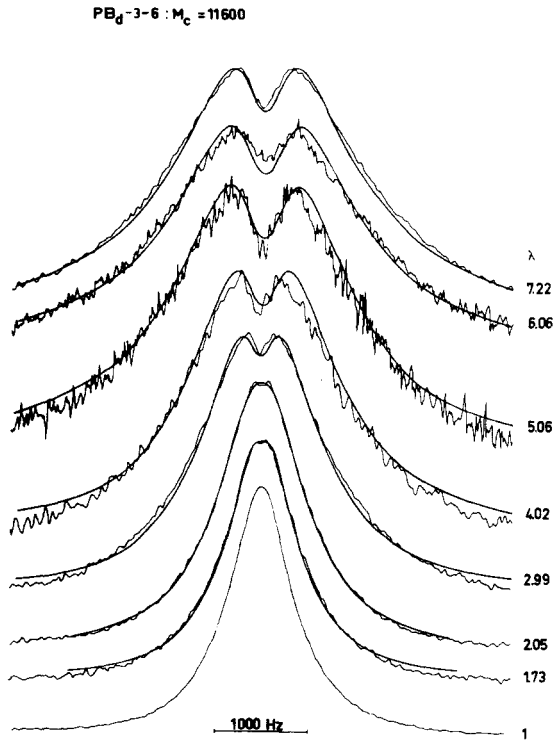

Figure 5. ^{2}H NMR spectra of sample PB_d-3-6 as a function of extension ratio λ and calculated spectra (see caption of Figure 3).

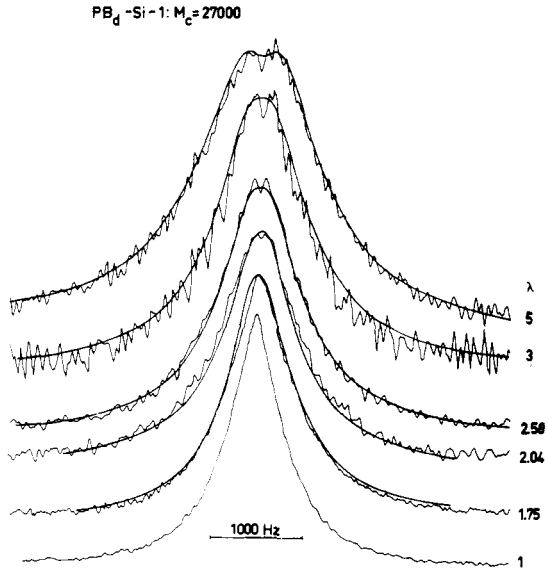

Figure 6. ^{2}H NMR spectra of sample BP_d-Si-1 as a function of extension ratio λ and calculated spectra (see caption of Figure 3).

tributed to the presence of a distribution of chain orientations which are not averaged by molecular motion. Motionally nonaveraged orientations can be rationalized in terms of a distribution of elastically effective chain lengths. In the affine deformation model the segments of short chains will be more strongly oriented than the segments of long chains because, according to eq 5 and 7, the segmental orientation increases with decreasing molecular weight of elastically effective chains which become oriented during extension. A most probable distribution of chain lengths and a Gaussian distribution were applied to simulate the spectral line shapes. The former is completely defined by the number-average molecular weight M_c, and the latter by M_c and the weight-average molecular weight M_w. Since dry networks are considered, the M_c values

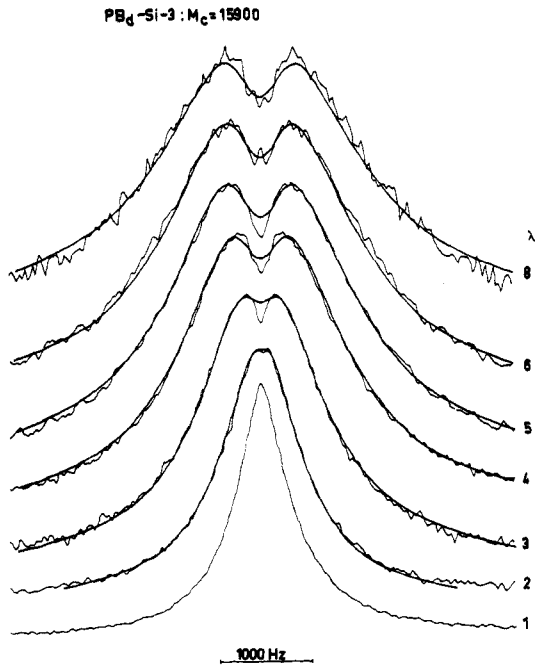

Figure 7. ^{2}H NMR spectra of sample PB_d-Si-3 as a function of extension ratio λ and calculated spectra (see caption of Figure 3.

determined from stress–strain measurements will be used. The analysis involves the calculation of the distribution $F_\lambda(\nu)$ of NMR frequencies $\nu = \pm\Delta\nu/2$ arising from different chains of the chain length distribution. $F_\lambda(\nu)$ is calculated for a given number of bonds per statistical segment n' and a given parameter $\langle P_2(\cos\Phi)\rangle_{app}$. The line shape function $I(\nu)$ fitted to the spectra then is the convolution of $F_\lambda(\nu)$ with the experimental line shape $L(\nu)$ of the isotropic sample, which is well approximated by a Lorentzian function; i.e.

$$I(\nu) = c\int_{-\infty}^{\infty} F_\lambda(\nu)L(\nu - \nu')\,d\nu' \qquad (8)$$

where c is a constant determined by the total area of the NMR resonance. The only parameters which enter the simulation procedure are $\langle P_2(\cos\Phi)\rangle_{app}$ and n'. As pointed out before, these parameters are not independent and n' is determined by the requirement of eq 6 such that $\langle P_2(\cos\Phi)\rangle_{app}$ is left as the only adjustable parameter.

Results

In Figures 3–7 the ^{2}H NMR spectra of the samples of Table I are shown. The smooth full lines were obtained with a most probable distribution of molecular weights, with the M_c values of Table I determined from mechanical measurements and the contribution of non-Gaussian terms in eq 5. In one case, PB_d-5-4 in Figure 3, the effect of a Gaussian distribution of chain lengths with $M_w/M_c = 1.9$ is shown for one extension ratio ($\lambda = 6$). This leads to a somewhat better approximation in the center of the doublet of signals. The most remarkable effect observed in all spectra is the increasing line width and intensity in the wings of the signals with increasing λ, which prevents fitting with a symmetrical Lorentzian line. This feature is satisfactorily reproduced by the distribution of chain lengths in conjunction with non-Gaussian chain statistics. The effect of chain length distribution is shown in more detail in Figure 8, where the frequency distribution $F_\lambda(\nu)$ can be directly compared to the most probable distribution $H(M)$ of chain molecular weights for sample PB_d-3-6. It can be seen that longer chains of the distribution contribute to the frequency distribution near the center of the

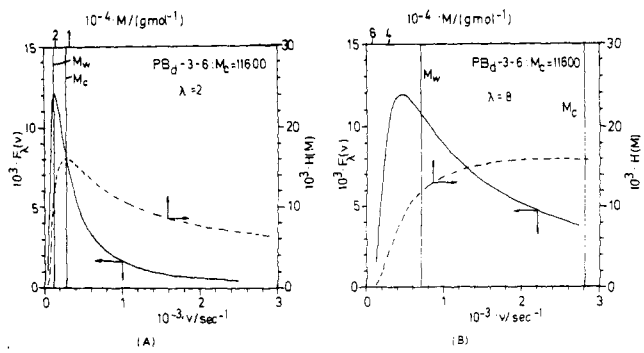

Figure 8. Calculated frequency distribution $F_\lambda(\nu)$ of quadrupolar splittings of the best fit to spectra of sample PB_d-3-6 and the corresponding most probable distribution $H(M)$ of network chain molecular weights at extension ratios $\lambda = 2$ and $\lambda = 8$. The calculation is based on eq 5, including non-Gaussian terms. Vertical lines indicate the location of the number-average molecular weight M_c and the weight-average molecular weight M_w of the chain length distribution.

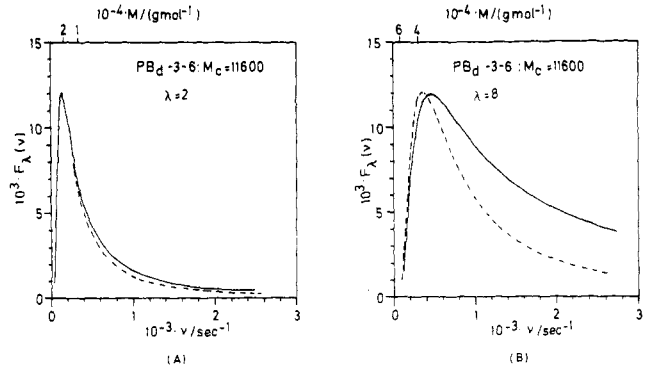

Figure 9. Frequency distributions of Figure 8 (full curves) and frequency distributions calculated with Gaussian chain statistics (dashed curves).

spectrum at $\nu = 0$, whereas short chains contribute to large quadrupolar splittings in the wings of the signals. For $\lambda = 2$ the contribution of M_w is located at the maximum of the frequency distribution, whereas M_c contributes at ca. $^2/_3$ of the maximum peak height of $F_\lambda(\nu)$. With increasing λ both molecular weight averages contribute increasingly to the declining part of the distribution, with M_n moving faster toward the edges than M_w. This is a consequence of the non-Gaussian terms in eq 5 becoming important for extension ratios $\lambda \gtrsim 3$. The effect of non-Gaussian chain statistics can be seen in Figure 9, where the frequency distributions with and without the higher order terms of eq 5 are shown for two extension ratios. The distribution of the Gaussian approximation was evaluated by fitting the calculated line shape as closely as possible to the experimental spectrum. As expected the Gaussian approximation fails to fit the wings of the spectral lines at large stretching ratios. In Figure 10 the best simulations obtained with Gaussian and non-Gaussian statistics are compared to the spectrum for $\lambda = 7.22$.

The simulated line shapes were calculated with the apparent C–D bond orientation parameter $\langle P_2(\cos\Phi)\rangle_{app}$. The condition of eq 6 requires that this parameter converge to the true orientation function $\langle P_2(\cos\Phi)\rangle_0$ of the unperturbed chains at vanishing deformation.[21] The number of bonds per statistical segment determined in this way is $n' = 40$ or 10 monomer units. The same value is obtained for every sample studied, independent of cross-link density, primary molecular weight, or position of the deuterium labels in the chain. The corresponding value of the orientation factor of the unstrained chains is $\langle P_2(\cos\Phi)\rangle = -0.154$.

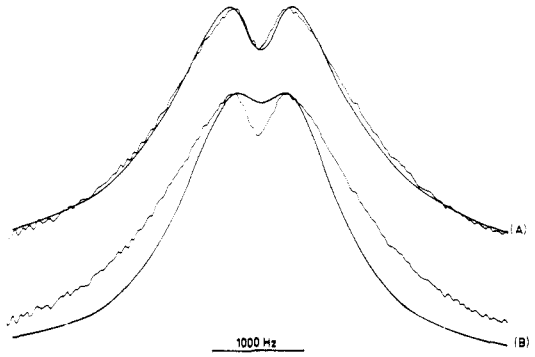

Figure 10. Spectrum of sample PB_d-3-6 at extension ratio λ = 7.22 and simulated spectra with non-Gaussian chain statistics (A) and Gaussian chain statistics (B).

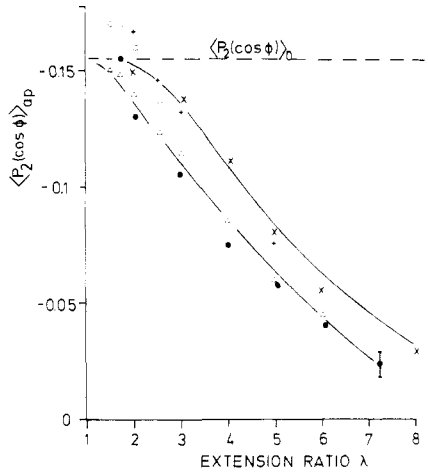

Figure 11. Apparent orientation function $\langle P_2(\cos\Phi)\rangle_{app}$ of methylene C–H bonds with respect to the end-to-end vector of the statistical segment as determined from the best fit to the spectra of the samples of Figures 3–7: (△) PB_d-5-4; (○) PB_d-3-5; (●) PB_d-3-6; (+) PB_d-Si-1; (×) PB_d-Si-3. $\langle P_2(\cos\Phi)\rangle_0$ is the orientation function of methylene C–H bonds with respect to the end-to-end vector of a statistical segment of 40 bonds as calculated for an unperturbed poly(1,4-butadiene) chain (cf. Figure 2).

When the spectra are fit with constant $n' = 40$, it turns out that the absolute value of the parameter $\langle P_2(\cos\Phi)\rangle_{app}$ decreases with increasing strain. This is shown in Figure 11 for all samples studied. The attempt to keep the parameter at a constant value $\langle P_2(\cos\Phi)\rangle_{app} = \langle P_2(\cos\Phi)\rangle_0$ by increasing the number of statistical segments n per chain, equivalent to an increase of M_c, failed. At high deformations the diminished frequency of short chains does not account for the spread of the intensity in the wings of the signals. The vertical line in Figure 11 at $\lambda = 7$ indicates the range of $\langle P_2(\cos\Phi)\rangle_{app}$ for an acceptable fit, corresponding to a change in M_c of only ±15%. Therefore, neither M_c nor n' (because of eq 6) can be varied to a significant extent without loss of quality of the spectral simulation. A further result of the calculations is that the $\langle P_2(\cos\Phi)\rangle_{app}$ parameters of the homogeneously deuterated networks and of the networks with deuterated junctions are approximately independent of the degree of cross-linking and of primary molecular weight and that the parameters of the latter are systematically greater than the parameters of the former.

In Figure 12 the quadrupolar splittings at peak height maximum are shown for both kinds of networks. The splitting first increases with increasing strain until a plateau value is reached. At moderate extensions ($\lambda \lesssim 3$), where effects from non-Gaussian statistics are small, the ratio of this splitting to the quantity $^3/_4\langle\delta\langle P_2(\cos\Phi)\rangle_{app}$ (cf. eq 3) can be considered as a measure of the segmental

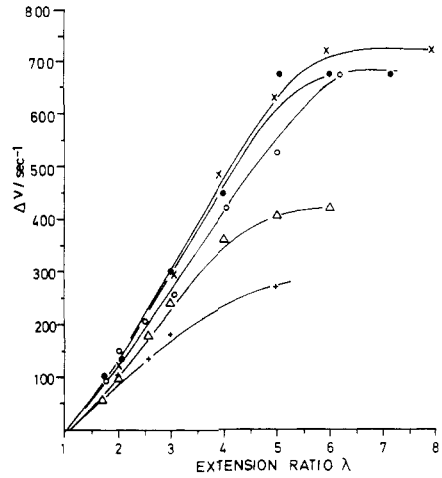

Figure 12. Quadrupolar splittings $\Delta\nu$ at maximum peak height of the spectra of Figures 3–7 as a function of extension ratio λ: (△) PB_d-5-4; (●) PB_d-3-6; (○) PB_d-3-5; (+) PB_d-Si-1; (×) PB_d-Si-3.

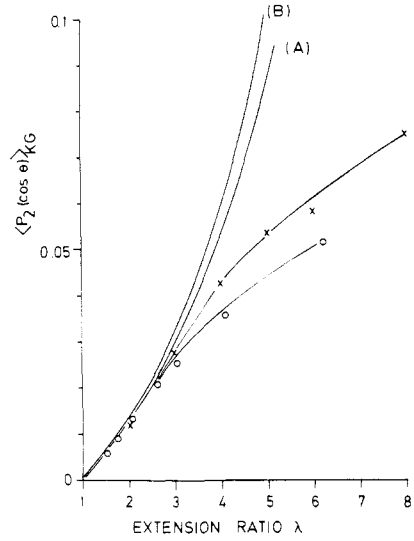

Figure 13. Kuhn–Grün orientation function $\langle P_2(\cos\Theta)\rangle_{KG}$ of the statistical segment as determined for the weight-average molecular weight M_w of the chain length distribution from the spectral simulations of two samples: (○) PB_d-3-5; (×) PB_d-Si-3. The two upper curves represent the theoretical orientation function calculated directly from eq 5 for Gaussian chain statistics (A) and non-Guassian chain statistics (B).

orientation function of chains with molecular weight near M_w (cf. Figure 8). Within the limits of accuracy of the measurements at small λ, the segmental orientation factor is inversely proportional to the number of statistical segments per chain n or M_c, respectively, in agreement with the prediction of the Kuhn–Grün theory. This holds for all kinds of networks of this study. For large strains the segmental orientation factor of a particular chain length can be determined on the basis of the Kuhn–Grün theory by the correspondence between chain length distribution and frequency distribution of quadrupolar splittings as shown in Figure 8. In Figure 13 the segmental orientation functions of chains with molecular weight M_w are shown for the homogeneously deuterated sample PB_d-3-5 and the sample PB_d-Si-3 with deuterated segments at network junctions. A comparison of these samples is particularly interesting because both have the same mechanical M_c of 15 900. For $\lambda \lesssim 3$ the segmental orientation is the same for both samples. However, for $\lambda > 3$ the orientation parameter of the sample with deuterated junctions becomes progressively greater with increasing strain than the orientation factor of the homogeneously deuterated net-

work. The slope of the curves decreases in a less abrupt manner than for the experimental quadrupolar splittings in Figure 12 and no saturation is observed. The segmental orientation function determined from the spectra can be compared to the theoretical orientation functions, which were calculated directly from eq 5 and 7 with the same values for M_w and n'. Both the Gaussian approximation (A) and the theoretical curve including non-Gaussian terms (B) are shown. Below $\lambda \sim 3$ the experimental orientation functions are well described by the theoretical $(\lambda^2 - \lambda^{-1})$ dependence of the Kuhn–Grün theory in the Gaussian regime. This behavior was also found for poly(dimethylsiloxane) networks in the dry state at small strains[3] and for the orientation of deuterated solvent molecules in strained swollen networks.[2] Above $\lambda \sim 3$ the experimental orientation function progressively lags behind the theoretical predictions.

Discussion

Figure 11 shows that the apparent orientation of methylene C–D bonds with respect to the end-to-end vector of the statistical segment increases from the negative value −0.154 of the unperturbed chain at small deformations toward the value of zero at large strains, which is the value for random orientation. According to calculations on stretched chains based on the RIS model,[19,22] which are valid for moderate extensions only, the absolute change of conformations on stretching and hence the change of the true bond orientation factor are very small. Independent of theoretical calculations, the change observed in Figure 11 is opposite to the expected strain dependence of the bond orientation function because the angles between methylene C–H bond directions and the vector of the statistical chain segment will be situated more frequently near 90° as the chains are stretched; i.e., the true orientation function is expected to decrease toward the value of −0.5 for perfect perpendicular orientation. Since significant variations of M_c or n' with λ can also be excluded, the only explanation of the observed peculiar dependence of $\langle P_2(\cos\Phi)\rangle_{app}$ on strain has to be seen in the failure of the Kuhn–Grün theory to describe the correct λ dependence of the segmental orientation function at higher strains. This could be already observed in the discrepancy between theoretical and experimental curves in Figure 13. Therefore, the variation of $\langle P_2(\cos\Phi)\rangle_{app}$ with λ is attributed to the λ-dependent part of the true segmental orientation function $\langle P_2(\cos\Theta)\rangle$. Proceeding in this way, it is assumed that the true bond orientation factor $\langle P_2(\cos\Phi)\rangle$ can be approximated by its value for the unstrained chain $\langle P_2(\cos\Phi)\rangle_0$ and that the true segmental orientation function has the same functional form as in the Kuhn–Grün theory. The procedure implies that in eq 5 an effective $\lambda^* < \lambda$ has to be used. Clearly, according to eq 3, the same fitting of the spectra is possible if $\Delta\nu$ is kept constant during this procedure.

Physically this means that elastically effective network chains are deformed less than the macroscopic dimensions, i.e., the deformation is nonaffine. In Figure 14 the molecular effective extension ratio λ^* of chains with molecular weight M_c and M_w is plotted vs. the macroscopic extension ratio λ for the homogeneously deuterated sample PB_d-3-5 and the sample PB_d-Si-3, which carries deuterium at network junctions only. Both networks are characterized by the same mechanical $M_c = 15900$. Above 200% extension the microscopically effective stretching ratio becomes progressively less than the macroscopical λ. In addition, it follows from the line shape analysis that the shorter M_c chains are stretched to a higher degree than the longer M_w chains. The difference between the effective

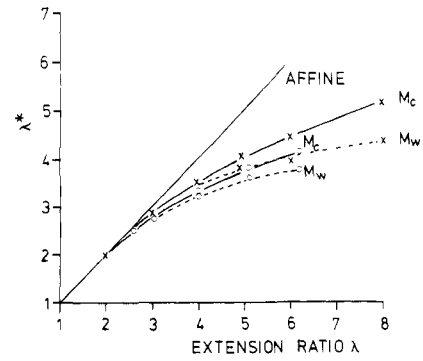

Figure 14. Molecular effective extension ratio λ^* vs. macroscopic extension ratio λ for the number-average molecular weight M_c and the weight-average molecular weight M_w of the chain length distribution from spectral simulations with constant parameter $\langle P_2(\cos\Phi)\rangle_{app} = \langle P_2(\cos\Phi)\rangle_0$ for two samples: (○) PB_d-3-5; (×) PB_d-Si-3.

extension ratios of both molecular weight averages increases with increasing deformation. The differentiation sets in where the non-Gaussian behavior becomes significant. Because the higher order terms in eq 5 depend on second and higher powers of the inverse of the molecular weight, a smaller reduction of λ is required for shorter chains to compensate for a constant $\langle P_2(\cos\Phi)\rangle$ term.

It could be argued that the smaller $\lambda^*_{M_w}$ with respect to $\lambda^*_{M_c}$ might be a consequence of the presence of dangling chain ends which are oriented less than elastically effective chains of the same length and therefore could depress the quadrupolar splitting in the high molecular tail of the chain length distribution. If this were true no difference would be observed between $\lambda^*_{M_w}$ and $\lambda^*_{M_c}$ for the junction deuterated network PB_d-Si-3, where dangling chains are not observable. This is not the case. The fact that for both kinds of networks the ratio of $\lambda^*_{M_w}$ and $\lambda^*_{M_c}$ is about the same shows that the contribution of dangling chain ends to the frequency distribution in Figure 8 occurs at smaller frequencies than the contribution of elastically effective chains of molecular weight M_w.

The nonaffine behavior of the networks as evidenced by the present ^2H NMR studies is in agreement with recent SANS experiments.[1] From the ^2H NMR line shape analysis it appears that the onset of the nonaffine deformation mechanism is connected with the non-Gaussian behavior, particularly of the shorter chains of the chain length distribution. Compared to SANS experiments on end-linked poly(dimethylsiloxane) networks with a narrow distribution of network chain lengths, the affine regime of the networks of this investigation, prepared by statistical cross-linking, appears to extend to higher extension ratios. This is probably due to the broader distribution of network strands and to the presence of entanglements in our networks, leading to a higher fraction of elastically effective short chains. The SANS experiments in fact show that the poly(dimethylsiloxane) network prepared from the lowest molecular weight precursor polymer approaches the affine behavior more closely than the networks prepared from longer precursor molecules.

The inhomogeneous nature of deformation of chains of different lengths emerging from the ^2H NMR experiments is a new feature. The idea that short chains become more extended during deformation has been put forward before,[23] but apparently no evidence on the basis of molecular properties has been presented up to now. The nature of inhomogeneous deformation of chains of different length has to be discussed in close conjunction with the nonaffine deformation mechanism. It has been proposed that individual network chains deform less than expected ac-

cording to the affine mechanism because due to rearrangements of network junctions and network unfolding, the distances of spatially neighboring network junctions may increase without similar changes of the dimensions of chains connecting topologically neighboring cross-links.[11] It has been pointed out that this mechanism will be of greater importance in networks prepared in solution, such as the samples in this study, because these networks contain fewer entanglements.[10] The proposed mechanism would also explain why networks prepared at higher dilution swell to a greater extent.[24,25] Entanglements cannot be completely avoided in a network that is statistically cross-linked in solution. This was demonstrated by the results of swelling measurements on the samples of this work.[5] In a loosely entangled solution made network, large translational motions of cross-links may still be possible. However, the presence of entangled short chains inevitably leads to progressively higher stretching of these chains, while longer chains will be lagging behind as the macroscopic strain increases. At sufficiently high extension ratios, the reservoir of long chains giving an additional contribution to overall orientation and storage of elastic energy on further stretching is being more and more depleted. This picture is consistent with the observed saturation of orientation of the chains in the high molecular weight tail of the chain length distribution, as indicated by the constancy of quadrupolar splittings at maximum peak height in Figure 12. In this respect, long unentangled chains play a similar role to that of dangling chain ends, which were also assumed to contribute to the small frequency range of the distribution of quadrupolar splittings. Saturation of orientation has also been observed in birefringence studies of rubbers at high extensions.[26] Contrary to these experiments, in which only the overall segmental orientation is probed, the ^2H NMR line shape analysis of deuterated elastomers affords an explicit distinction of the orientational behavior of different parts of the distribution of elastically and orientationally effective chains.

As Figure 11 shows, the fitting parameter $\langle P_2(\cos \Phi)\rangle_{app}$ is systematically greater for the networks deuterated at network junctions than for the homogeneously deuterated networks. Accordingly, the effective molecular stretching ratios λ^* in Figure 14 are greater for the former networks than for the latter. The enhancement is the same for both M_w and M_c chains. In light of the preceding discussion, this effect is attributed to the orientational properties of elastically effective chains and not to dangling chain ends. It is interpreted by an inhomogeneous deformation of chains along their contour length, giving rise to an excess orientation and higher effective stretching of chain segments which are bound to network junctions. Apparently, the inhomogeneous deformation of individual chains becomes effective only at higher strain where deviation from affine behavior is also observed. The extent of inhomogeneous deformation increases with increasing strain. This seems to contradict current ideas on rubber elasticity, according to which the constraints to which network junctions are subjected are assumed to decrease with increasing strain.[9]

Concluding Remarks

It should be remarked that the conclusions concerning the nonaffine and inhomogeneous nature of chain deformation are based on the validity of the interpretation of the changes of ^2H NMR line shapes on deformation in terms of motionally nonaveraged orientations from different parts of the distribution of elastically and orientationally effective chains in the network. In a recent ^2H NMR study of a fully deuterated poly(dimethylsiloxane) network it has been suggested that the spread of the spectral wings with increasing strain might be a consequence of the presence of deuterons with different dynamical behavior, although this was not studied in detail.[3] Further experiments will be carried out to elucidate this point. For this purpose networks are being prepared under identical conditons from star molecules with deuterium-labeled segments at topologically defined sites: at chain ends, in the middle of the chains, and at the star centers. In particular, appropriate ^2H NMR relaxation studies, e.g., spin alignment,[14] and quasi-elastic neutron scattering experiments on junction deuterated systems are being planned with the objective of investigating the fluctuation of network junctions as a function of strain.

Acknowledgment. These studies were rendered possible by the NMR equipment placed at our disposal by the Bundesministerium für Forschung und Technologie. The work was furhter supported by the Deutsche Forschungsgemeinschaft, Sonderforschungsbereich 60. M.M.J. gratefully acknowledges a grant from CAPES, Ministry of Education, Brazil.

References and Notes

(1) Candau, S.; Bastide, J.; Delsanti, M. *Adv. Polym. Sci.* **1982**, *44*, 27.
(2) Deloche, B.; Samulski, E. T. *Macromolecules* **1981**, *14*, 575.
(3) Deloche, B.; Beltzung, M.; Herz, J. *J. Phys. (Paris) Lett.* **1982**, *43*, 763.
(4) Stein, R. S. *Rubber Chem. Technol.* **1976**, *49*, 458.
(5) Stadler, R.; Maldaner Jacobi, M.; Gronski, W. *Makromol. Chem., Rapid Commun.* **1983**, *4*, 129.
(6) Flory, P. J. "Principles of Polymer Chemistry"; Cornell University Press: Ithaca (NY) and London, 1953.
(7) James, H. M. *J. Chem. Phys.* **1947**, *15*, 651.
(8) James, H. M.; Guth, E. J. *J. Chem. Phys.* **1947**, *15*, 669.
(9) Flory, P. J. *J. Chem. Phys.* **1977**, *66*, 5720.
(10) Ullman, R. *Macromolecules* **1982**, *15*, 582.
(11) Bastide, J.; Picot, C.; Candau, S. *J. Macromol. Sci., Phys.* **1981**, *B19*, 13.
(12) Abragam, A. "The Principles of Nuclear Magnetism"; Oxford University Press: New York, 1961.
(13) Hentschel, D.; Sillescu, H.; Spiess, H. W.; Voelkel, R.; Willenberg, B. *Magn. Reson. Relat. Phenom., Proc. Congr. Ampere, 19th* **1976**, 381.
(14) Spiess, H. W. *Colloid Polym. Sci.* **1983**, *261*, 193.
(15) Collignon, J.; Sillescu, H.; Spiess, H. W. *Colloid Polym. Sci.* **1981**, *259*, 220.
(16) Cope, A. C.; Berchtold, G. A.; Ross, D. L. *J. Am. Chem. Soc.* **1961**, *83*, 3859.
(17) Cookson, R. C.; Gupte, S. S.; Stevens, J. D. R.; Watts, C. T. *Org. Synth.* **1971**, *51*, 121.
(18) Treloar, L. R. G. "The Physics of Rubber Elasticity"; Clarendon Press: Oxford, 1975.
(19) Abe, Y.; Flory, P. J. *Macromolecules* **1971**, *4*, 219.
(20) Kuhn, W.; Grün, F. *Kolloid Z.* **1942**, *101*, 248.
(21) Since the sign of the quadrupolar splitting cannot be determined, only the absolute value of $\langle P_2(\cos \Theta)\rangle_{ap}$ is obtained. The sign follows from eq 6.
(22) Abe, Y.; Flory, P. J. *J. Chem. Phys.* **1970**, *52*, 2814.
(23) Rehage, G. *Pure Appl. Chem.* **1974**, *39*, 161.
(24) Alfrey, T., Jr.; Lloyd, W. G. *J. Polym. Sci.* **1962**, *62*, 159.
(25) Lloyd, W. G.; Alfrey, T., Jr. *J. Polym. Sci.* **1962**, *62*, 301.
(26) Doherty, W. O. S.; Lee, K. L.; Treloar, L. R. G. *Br. Polym. J.* **1980**, 19.